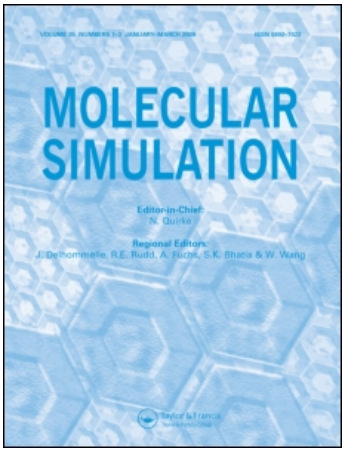

Molecular Simulation
Publication details, including instructions for authors and subscription information:
http://www.informaworld.com/smpp/title~content=t713644482

Theoretical investigation of the electronic coupling element in bis-ruthenium porphyrin dimers

S. Pheasant[a]; J. A. Kouzelos[a]; H. Van Ryswyk[a]; R. J. Cave[a]
[a] Department of Chemistry, Harvey Mudd College, Claremont, CA, USA

To cite this Article Pheasant, S. , Kouzelos, J. A. , Van Ryswyk, H. and Cave, R. J.(2006) 'Theoretical investigation of the electronic coupling element in bis-ruthenium porphyrin dimers', Molecular Simulation, 32: 9, 677 — 693
To link to this Article: DOI: 10.1080/08927020600863717
URL: http://dx.doi.org/10.1080/08927020600863717

Molecular Simulation, Vol. 32, No. 9, 15 August 2006, 677–693

Taylor & Francis
Taylor & Francis Group

Theoretical investigation of the electronic coupling element in bis-ruthenium porphyrin dimers

S. PHEASANT†, J. A. KOUZELOS, H. VAN RYSWYK‡ and R. J. CAVE*

Department of Chemistry, Harvey Mudd College, 301 Platt Boulevard, Claremont, CA 91711, USA

(Received March 2006; in final form May 2006)

The electronic coupling element for electron transfer is studied in three ruthenium-porphyrin dimers. The dimers are models for compounds that have been previously studied experimentally and allow investigation of orientation effects and linkage effects and comparison of axial ligand effects on the electronic coupling. The geometries used in this study were obtained from B3LYP geometry optimizations in a DZ basis, and the coupling element was calculated as half the energy splitting between pairs of symmetry-related orbitals using Hartree–Fock, B3LYP Kohn–Sham, or INDO orbitals. The results suggest that all three methods give qualitatively similar values of the coupling at a given geometry and that the coupling involving the highest occupied molecular orbital can be changed markedly by changes in orientation or by changes in ligation external to the main pathways for coupling. Following discussion of the results we suggest directions in which future methodological developments will be critical in furthering our ability to understand and predict electron transport.

Keywords: Electronic coupling element; Creutz–Taube ion; Ruthenium-porphyrin dimers; Compounds

1. Introduction

Significant strides have been made in recent years in the understanding and control of charge transfer in synthetic and naturally occurring systems [1,2]. The roles played by inner- and outer-sphere reorganization and reactant and product free energy differences were elucidated by Marcus [3] and Hush [4] and elaborated to include quantum mechanical effects by Levich [5], Dogonadze [6], Jortner [7], and others [8]. More recent work has provided an understanding of how differing timescales in subsystem dynamics can alter reaction rates [8–10]. Thus at present a relatively detailed picture exists to treat medium and energetic effects on the rate of electron transfer.

The earliest quantum mechanical treatments of the electron transfer process also pointed to the importance of the actual electron tunneling event [5,11–13] in controlling the rate. In semiclassical treatments of electron transfer this effect is included via a Landau–Zener curve crossing model [13], leading to a rate expression of the form

$$k(R_{\mathrm{DA}}) = \frac{2\pi}{\hbar}\frac{|H_{DA}|^2}{(4\pi\lambda kT)^{1/2}}\exp(-\Delta G^{\dagger}) \qquad (1)$$

where λ is the reorganization energy, $\Delta G^{\dagger}$ is the free energy of activation, and H_{DA} is the electronic coupling element for electron transfer. While the reorganization energy and free energy of activation are distance-dependent, it is the electronic coupling element that is responsible for the predominant distance- and orientation-dependence of the rate and thus it has received considerable attention [14–22]. Since the electronic coupling decays exponentially with distance between the donor and acceptor it gives rise to a sharp decrease in rate with distance [23], but its orientation dependence at fixed distance can also be quite dramatic [24–27]. It has also been shown in many contexts that the coupling is sensitive to the intervening medium between the donor and acceptor [12,17,18,28–31] and large variations in the

*Corresponding author. Email: robert_cave@hmc.edu
†Present address: Department of Chemistry, Rice University, P.O. Box 1892, MS-60, Houston, TX 77251, USA.
‡Email: hal_vanryswyk@hmc.edu

Molecular Simulation
ISSN 0892-7022 print/ISSN 1029-0435 online © 2006 Taylor & Francis
http://www.tandf.co.uk/journals
DOI: 10.1080/08927020600863717

coupling and its distance dependence can be observed as a function of the medium through which the electron tunnels. While this sensitivity can at times be an impediment to achieving maximal reaction rates it can also be viewed as another tool available for control and manipulation of the relative rates of reaction in naturally occurring or synthetic systems.

One area where an understanding of the electronic coupling will play a crucial role is in the developing field of nanoelectronics [2]. As the drive towards nanoscale electronic devices accelerates, the question of selection and design of the optimal components for construction of such devices arises. Synthetic ease, robustness and efficiency are obvious primary concerns, but the ability to control the relative rates in these systems to achieve optimal charge transport is in the end the fundamental issue that will determine their usefulness. Because of its strong orientation dependence the electronic coupling element is a potentially important means of altering rates with modest motions of the subcomponents of such devices.

A number of groups have taken their queue from electron transport chains found in nature and investigated the use of porphyrins (Por) and Por derivatives in synthetic charge transfer systems [32–35]. Por have the advantages of stability, relatively low outer sphere and inner sphere reorganization energies when undergoing charge transfer, ease of manipulation of their redox potential (either by metal substitution or addition of substituents to the ring), and a relatively rich history of prior study to guide the direction of future design. Several groups have previously examined the electronic coupling in electron transfers involving Por, including Siders *et al.* [25–27] and Friesner and coworkers [36].

Early experimental work with metalloporphyrin oligomers focused on the concept of molecular wires [37,38], with more recent studies directed towards the production of supramolecular rods [39,40]. Metalloporphyrin oligomers can be used as self-assembling blocks to make discrete, ordered arrays of metalloporphyrins [41,42], or combined with other molecules to create larger structures. These supramolecular structures have utility as sensors [43] and as constituents of specifically designed nanoporous materials [44,45], in addition to exhibiting electronic properties unique to fully π-conjugated systems of this size [46,47]. Metalloporphyrin oligomers also have interesting magnetic properties [48].

In the realm of biomimetic models, metalloporphyrin oligomers have been used to imitate bacterial photosynthetic reaction centers [49], or to form the basis for light-harvesting complexes, comprising modular, 2–100 nm photonic building blocks that may be combined to produce supramolecular structures with finely-tuned optical properties [50].

Finally, metalloporphyrins catalyse a wide range of chemistry, both in nature and *in vitro*. Metalloporphyrin oligomers hold the promise to tailor the catalytic power of metalloporphyrins in new systems [51].

With this in mind we have been engaged in combined experimental and theoretical studies of a series of linked ruthenium (Ru)-Por. The present article is a first step in treating them from a theoretical perspective, and to our knowledge is the first treatment of the electronic coupling involving Ru-Por.

Several issues arise when considering the electronic coupling in systems of this type. First, the question of the appropriate level of theoretical treatment is obviously critical. Small model systems can be treated using a variety of high-level quantum chemical methods [29,30] allowing one to assess the relative accuracy of more approximate techniques. In systems involving Por it is not currently possible to treat these at what might be considered a "state of the art" level, thus at present our results will need to be judged on the basis of internal consistency and agreement with experiment where comparisons can be made. A second important question concerns the sensitivity of the coupling to the intervening medium between the donor and acceptor. We explicitly control/define the intervening medium in these systems by covalently bonding the donor and acceptor in relatively rigid arrangements, but the question of how thermal fluctuations and unbound solvent might alter the predictions made here will need to be addressed [52]. Finally, the question of which of the calculated states of the donor and acceptor correspond to the initial and final states of the electron transfer event one might observe experimentally is also critical. The accurate determination of the relative ordering of the low-lying states is further complicated where solvent effects and inner sphere reorganization are neglected.

In the present study we begin the theoretical treatment of Ru-Por oligomers, addressing questions that are relatively general in nature. Our hope is that the answers to these broader questions may be less dependent on theoretical details but will still be of use in the further design of systems of this type. In particular, we focus on three distinct bis-Ru-Por complexes, shown in figure 1. The first is a cofacial dimer (figure 1(A)), linked by pyridine (py) coordination to the ruthenium in each Por ring, capped externally by carbonyl ligands. The dimer has been synthesized and studied experimentally by Funatsu *et al.* [53] as well as our own group. The second is a pyrazine (pz) linked "linear" dimer (figure 1(B)), with carbonyls as capping ligands on the external faces of the Por rings. The third dimer is another pz-linked structure, with py caps rather than carbonyl ligands (figure 1(C)). For comparison we have also performed similar calculations on the Creutz–Taube ion [54–56] (a well-studied bis-ruthenium pz-linked complex) (figure 1(D)).

The questions we seek to address in the present study are:

(1) How sensitive are the computed couplings to the theoretical methods used to describe the system?
(2) How sensitive are the couplings to the orientation of the Por rings and the mode by which they are linked?

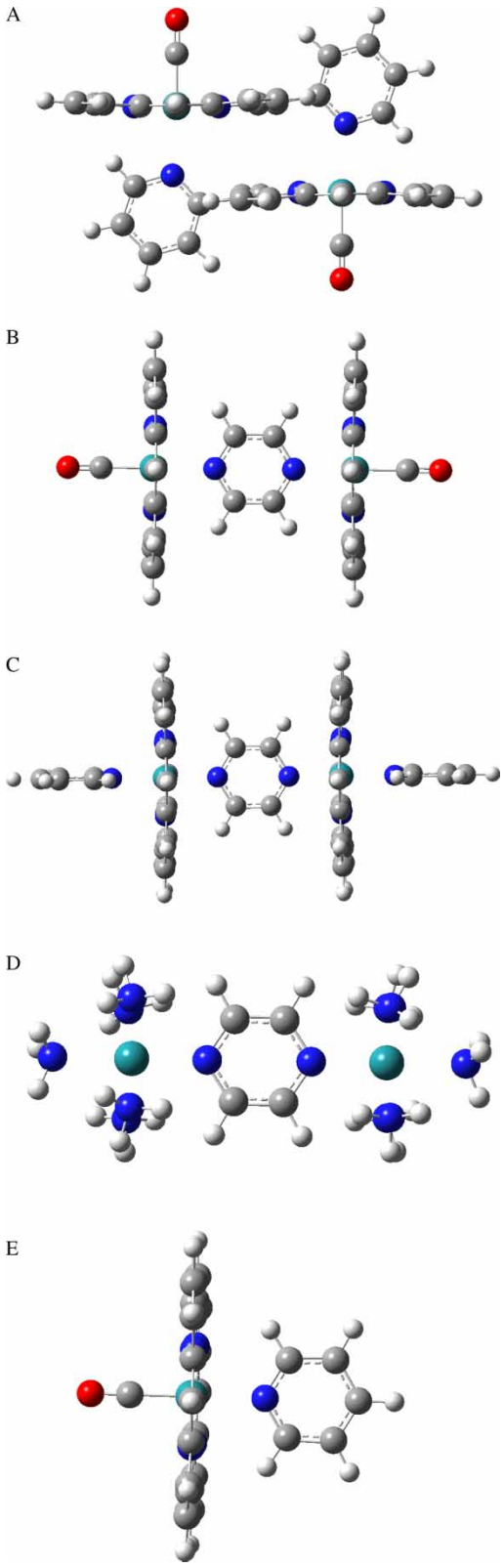

Figure 1. Complexes investigated in the current study. (A) The cofacial Ru-Por dimer; (B) the linear bis-CO Ru-Por dimer; (C) the linear bis-py Ru-Por dimer; (D) the Creutz–Taube ion; (E) the Ru(Por)(CO)(py) monomer.

(3) Do the external ligands play a significant role in controlling the coupling?
(4) Can energetic effects be used to control the effective coupling in systems of this type?

The results presented below suggest that the conclusions drawn for the coupling in these systems are only modestly affected by the theoretical method used for their description and that changes in orientation and distance can have a dramatic effect on the coupling. Perhaps most surprising is that the effective coupling in these systems can be dramatically altered by the choice of capping ligand, largely through a change in the nature of the HOMO in the complex.

The remainder of the paper is organized as follows. In the following section we discuss the theoretical methods used to describe the systems and to calculate the electronic coupling element for electron transfer. In the third section we present our results for the coupling and follow that with a discussion of the results. In the fifth section we discuss future directions the field will need to take in order to treat the electronic coupling in systems of this type with the accuracy needed to guide experiment. We then end with conclusions.

2. Theoretical methods

Structures for each dimer and the Creutz–Taube ion were obtained from density functional theory (DFT) B3LYP [57] geometry optimisations in a DZ basis. This basis corresponds to use of the Los Alamos effective core potential and associated DZ basis for Ru [58], while all other atoms were treated at the all-electron level using the Dunning valence DZ basis [59]. Initial dimer geometries were optimized in C_1 symmetry and these structures were then used to construct a symmetrical geometry which was further optimized in higher symmetry. Similar calculations were performed for a neutral Ru-Por monomer with CO and py as fifth and sixth ligands (Ru(Por)(CO)(py)) (Figure 1(E)). Reasonable agreement between experiment and theory was obtained for the Ru-ligand bond lengths (experimental results were for a Ruthenium tetraphenylporphyrin complex with CO and py axial ligands [60]: calculated $Ru-N_{py} = 2.216$ Å; experimental $Ru-N_{py} = 2.193$ Å; calculated $Ru-C_{CO} = 1.866$ Å; experimental $Ru-C_{CO} = 1.838$ Å). Each dimer was optimized as a neutral species, while the Creutz–Taube ion was optimized as the +4 ion.

The electronic coupling element can be calculated in a variety of ways [2]. In the present study we used the Koopmans' Theorem (KT) approximation to calculate H_{DA} [21,22,61,62], using the orbital energies of the neutral complex (or +4 ion for the Creutz–Taube ion) at the (symmetrical) optimized geometry (electronic coupling equals half the orbital energy difference). These one-electron states occur as plus/minus combinations of orbitals localized on the individual Por rings (with contributions from the linking and external ligands as well, where allowed by symmetry). This approximation has been used in a number of previous studies [21,22,30,62–64]. In essence, one is assuming the adiabatic states at the transition state for the charge transfer process can be represented by removal of an

electron from a single orbital of the neutral complex (i.e. that there is little differential electronic relaxation of the remaining orbitals upon ionization of the complex) and thus that the difference in orbital energies is a good approximation to the difference in ionization potentials one would obtain using many-electron techniques [65–70]. In one case below we compare these results with many-electron results to investigate relaxation effects and find good agreement where the comparisons can be made. Of course, the geometry used, while symmetrical, is not that of the actual transition state of the charge transfer process in the cations. However, to the extent that the Condon approximation is valid (i.e. the coupling is weakly dependent on nuclear geometry) a similar result should be obtained at the symmetrical geometry of the neutral species.

This approach restricts us from considering photo-excited electron transfer processes and low-energy thermal reactions involving orbitals that are not symmetry-related on the two centers, which would be possible if many electron descriptions could be obtained and used in the generalised Mulliken–Hush (GMH) approach [69,70]. We are in the midst of implementing a one-electron version of the GMH method based on KT [71,72] that will allow us to examine non-symmetry related and photo-excited transfers and hope to explore them in these systems in the near future.

In summary, given a geometry for the neutral molecule obtained as described above, we then calculated the electronic coupling element for charge transfer in the mono-cations of these dimers based on the orbital energy differences obtained in calculations of the neutral dimers. We estimate that our results are converged to within $2\,cm^{-1}$. We have described the systems using: (a) Restricted Hartree–Fock (RHF) theory; (b) the semiempirical Intermediate Neglect of Differential Overlap (INDO) approach using the Zerner group parameterization; and (c) DFT using the B3LYP functional (using the Kohn–Sham (KS) orbital energies). Note, in the case of DFT there is no direct analogue of KT, and only the HOMO energy has a rigorous interpretation [73]. However, previous calculations have shown that the Kohn–Sham orbital energy differences can give results comparable to RHF–KT or all-electron couplings, at least for moderate distances [21]. Recent work in the Baerends group [74] suggests that the KS orbital energies are good approximations to relaxed atomic or molecular ionization potentials, suggesting their use in electronic coupling calculations in much the same way as the HF orbital energies are used. Our results suggest the B3LYP functional yields results in good agreement with the other two methods considered here.

The size of the DZ basis is relatively modest, particularly for long-range electron transfer. One might fear that it is insufficient to treat the transfers between Ru-Por localized orbitals in the linear dimers since it does not have functions optimized to reproduce the long-range behavior of the relevant atomic orbitals at these distances. However, the pz linaer possesses unoccupied orbitals that can be used to partially offset this basis set incompleteness, as has been found in studies of linear alkanes [21,63]. Thus we expect that the couplings will not be as sensitive to the use of a small basis as they would be if there were no linker present. We present results below for the linear bis-CO dimer that assess the impact of addition of diffuse functions and see modest effects. As a result we have not included them for the other complexes studied.

All DFT geometry optimisations and all HF or B3LYP orbital energy calculations were performed using Gaussian 98 [75] or Gaussian 03 [76]. Orbital plots and rendering for HF and KS orbitals were done using Gaussview 2 or 3. The INDO calculations were done using the MSI implementation [77] of the Zerner group code [78].

3. Results

The geometries of the four complexes investigated here are presented in figure 1 (detailed geometrical information is provided in Appendix I). In each case the py or pz ligands bisect the N–Ru–N angles of either the Por or the Creutz–Taube ion's equatorial ligands. We performed a test calculation on the bis-CO dimer to search for a stationary point having the pz plane oriented along the line formed by a pair of *trans*-N atoms in the Por ring. Convergence was slow and the structure was at least 1.5 kcal/mole above the structure shown in figure 1(B), thus we did not consider these geometries further. None of the conclusions drawn below are likely to be affected were structures of this type examined. The cofacial diporphyrin (figure 1(A)) exhibits a modest amount of ring puckering, but the Por rings in the two linear dimers (figure 1(B),(C)) are essentially planar. Some relevant bond lengths for the various structures are given in table 1. The structures were optimized in C_2 symmetry (cofacial, bis-CO, and Creutz–Taube ion) and C_S symmetry (bis-py). In all cases except for the bis-CO complex the given symmetry gave symmetric/anti-symmetric orbital pairs that belonged to different irreducible representations. In

Table 1. Selected bond lengths for various structures*.

Complex	*Ru–N$_{por}$*†	*Ru-ligand*‡	*Ru–N$_{py/pz}$*¶	*Ru–Ru*
Cofacial	2.081	1.837	2.428	6.518
Bis-CO	2.081	1.868	2.200	7.217
Bis-Py	2.070	2.125	2.089	7.020
CT	2.209	2.216	2.117	7.146

* All lengths in Å. † Average of the four Ru–N bond lengths. ‡ Bond length between Ru and external ligand. For the cofacial and bis-CO compounds this is the Ru–C_{CO} bond length, while for bis-py it is the Ru–N_{py} bond length. ¶ In the cofacial complex this is the Ru–N_{py} length, while in the remaining three compounds it is the Ru–N_{pz} length.

the bis-CO case the C_2 axis was assigned as the long axis of the molecule, and thus the symmetric and anti-symmetric pairs of orbitals did not belong to different irreducible representations. Nevertheless, the final optimized structure possessed C_2 symmetry with respect to rotation about a symmetry axis perpendicular to the long axis of the molecule to within 0.0001 Å in all coordinates, and we used the pairs of orbitals correlating with the symmetric and anti-symmetric pairs (were full symmetry present) to obtain coupling elements as described above. A test calculation was performed where the bis-CO complex was reoptimized (B3LYP, DZ basis) in D_{2h} symmetry and it yielded coupling elements using KS orbital energy differences within a wave-number of those based on the C_2 optimized structure considered here.

We focus on the couplings involving the four highest occupied molecular orbitals of the Ru-Por monomers from which the dimers arise. These orbitals are shown in figure 2 for the monomer Ru(Por)(CO)(py). While modest changes in their shapes are expected if the CO or py are removed/replaced, these are essentially the shapes observed in all three Ru-Por dimers. With only the Por ligand present the structure would be D_{4h}. The complexes studied here have significantly lower symmetry than D_{4h} but we will refer to the orbitals based on their irreducible representations were the structure D_{4h}. Thus, the HOMO in the Ru(Por)(CO)(py) monomer correlates with an orbital of A_{2u} symmetry, while the HOMO-1, HOMO-2 and HOMO-3 correlate with A_{1u} and E_g orbitals (and we will refer to these as d_1 E_g and d_2 E_g, respectively). It is seen that the A_{1u}

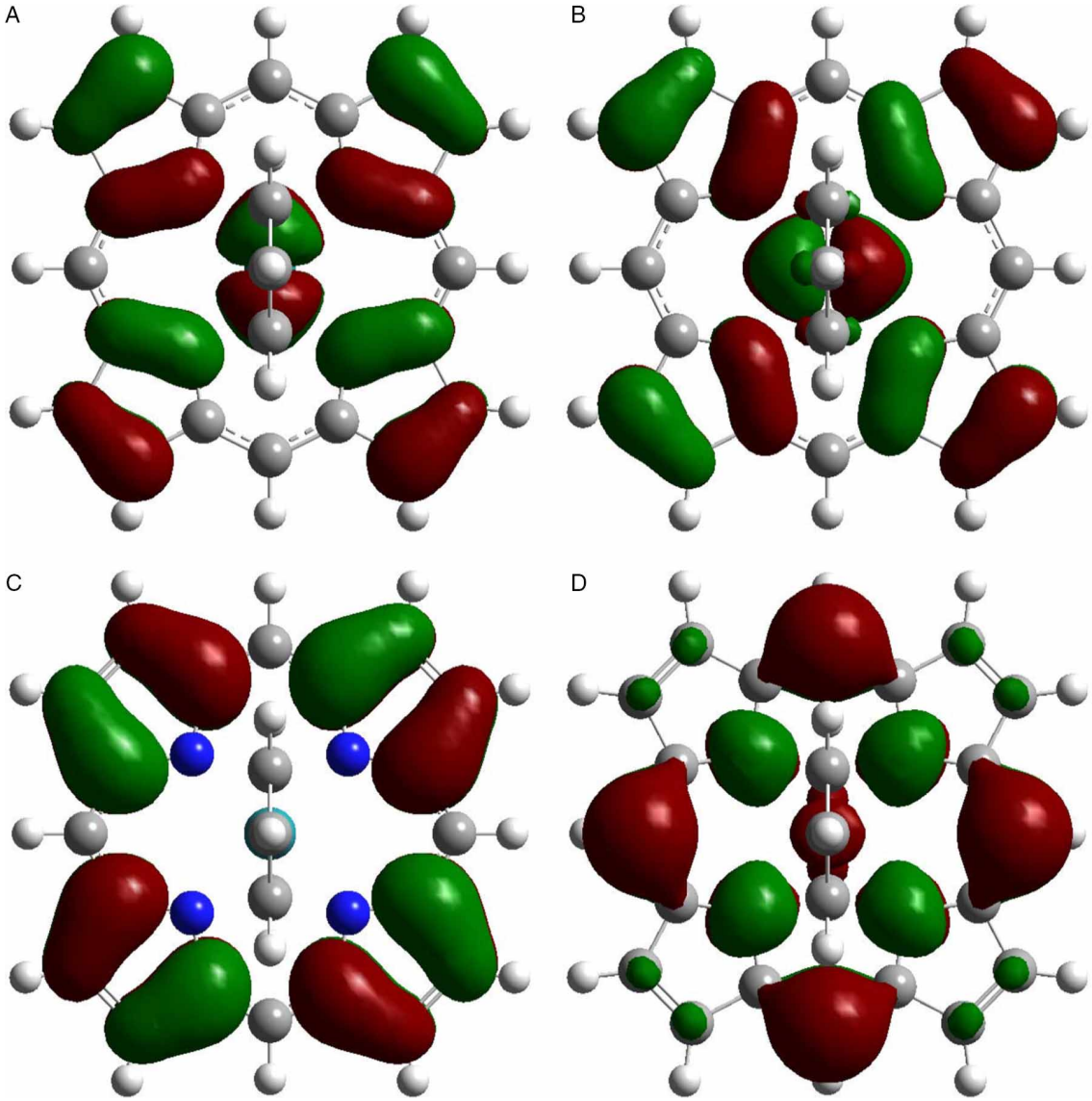

Figure 2. The four high-lying molecular orbitals considered in the present study. The orbitals are the four highest-lying KS orbitals from a B3LYP calculation on the Ru(Por)(CO)(py) monomer. (A) d_2 E_g HOMO-3; (B) d_1 E_g HOMO-2; (C) A_{1u} HOMO-1; (D) A_{2u} HOMO.

Table 2. Coupling elements for the cofacial complex[†].

Orbital	*DFT* orbital pair ε_{avg}	*HF* orbital pair ε_{avg}	*INDO* orbital pair ε_{avg}
A_{1u}	487	590*	756*
	H-1, H-3	H, H-1	H, H-1
	−5.3	−6.2	−6.5
A_{2u}	491*	488	240
	H, H-2	H-2, H-3	H-2, H-3
	−5.3	−6.6	−6.9
d_1 E_g	407	780	680
	H-5, H-7	H-4, H-7	H-4, H-7
	−5.65	−8.4	−7.6
d_2 E_g	270	430	402
	H-4, H-6	H-5, H-6	H-5, H-6
	−5.63	−8.4	−7.55

[†] In each case we present couplings in cm^{-1} between the pair of orbitals of the given local D_{4h} symmetry, indicating what orbital number they correspond to in the dimer (H-1 is the HOMO-1 orbital, for example), and the average orbital energy ε (in eV) of the symmetric/anti-symmetric orbital pair, based on the eigenvalues of the Kohn–Sham (DFT) or Fock (HF, INDO) operators. The coupling element involving the HOMO of the complex for each method is indicated by *.

Table 3. Coupling elements for the bis-CO complex[†].

Orbital	*DFT* orbital pair ε_{avg}	*HF* orbital pair ε_{avg}	*INDO* orbital pair ε_{avg}
A_{1u}	<5	6*	9*
	H-2, H-3	H, H-1	H, H-1
	−5.6	−6.45	−6.7
A_{2u}	29*	10	10
	H, H-1	H-2, H-3	H-2, H-3
	−5.4	−6.7	−6.9
d_1 E_g	343	272	627
	H-4, H-7	H-4, H-5	H-4, H-7
	−5.78	−8.54	−7.75
d_2 E_g	16	29	15
	H-5, H-6	H-6, H-7	H-5, H-6
	−5.77	−8.56	−7.75

[†] See table 2 for definitions. In this case, the d_1 E_g orbitals have the proper symmetry to interact with the pz π orbitals, while the d_2 E_g orbitals are orthogonal to the pz π orbitals.

and A_{2u} orbitals contain no metal character and are delocalised over the Por ring, whereas the E_g pair contains significant metal character. The pair of axial ligands each allow delocalisation from the metal onto the ligands, with the py interacting strongly only with the metal orbital (denoted d_1) that is π-like with respect to the py plane, whereas in the case of CO, both metal orbitals can delocalise into the π* CO orbital.

In table 2 we present results for the coupling elements for these four orbital pairs in the cofacial compound. The coupling elements for each of the four orbitals of interest are in the range of several 100 cm^{-1}, independent of theoretical method. In all cases except that of the DFT d_1 E_g pair the high-lying orbitals were plus/minus combinations of orbitals quite similar to those shown in figure 2. For the DFT d_1E_g pair the orbitals had similar shapes to those of figure 2(B) at and near the metal on the Por ring, but the nodal structure departed somewhat from that of figure 2(B) on the outer portions of the ring. We attribute these deviations to the close contact of the two rings. In none of the other complexes considered below do we see significant deviations from the monomer orbital shapes given in figure 2. Given the size of these complexes and the modest reorganisation energies expected these coupling elements suggest that the charge transfer would fall in or near the adiabatic regime, independent of which orbital corresponds with the actual HOMO of the complex. There is reasonable agreement for the coupling values between the various methods (generally within a factor of two, and frequently better). Examining the average orbital energies ε it is seen that all methods predict that the metal-containing orbitals (E_g here) fall somewhat below the energies of the A_{1u} and the A_{2u} orbitals, although the difference in energy between these two sets of orbitals is strongly method-dependent. As noted above, there are questions associated with the interpretation of the Kohn–Sham orbital energies other than that for the highest KS orbital. Furthermore, the orbital energies obtained from approximate density functionals are generally shifted to higher energies than those expected from the exact functional [79]. Thus, in the present work we will focus on trends associated with the relative energies of these four orbitals, as well as the couplings obtained from them, but will be somewhat more reserved when it comes to using our theoretical results alone to decide the character of the orbital pair involved in *et* in the ground state complex. In the discussion section we address this issue again using data from previous experiments on these systems and are then able to be somewhat more definite with respect to the nature of the lowest state of the ion. In the present case, however, all three methods indicate that the likely orbitals involved in thermal *et* in the ground state of the cofacial dimer are largely non-metal containing (i.e. A_{1u} or A_{2u}).

Table 3 contains our results for the bis-CO complex. The A_{1u} and A_{2u} orbitals are again found to be highest-lying for all methods and the coupling elements are generally quite similar for a given orbital pair for all three methods. Unlike the cofacial complex, in this case we find large coupling only for the d_1 E_g pair of orbitals. This is not surprising in that the Por–Por inter-plane separation has increased considerably relative to the cofacial complex (despite the fact that the Ru–Ru distances are similar). All three methods are in agreement that the coupling between the A_{1u} and A_{2u} orbitals on either centre are relatively small, and lie most likely in the non-adiabatic regime. The coupling predicted for the d_1 E_g pair of orbitals is of comparable size to those seen for the cofacial complex, but the coupling for the d_2 E_g pair of orbitals is predicted to be

Table 4. Coupling elements for the bis-py complex†.

Orbital	*DFT orbital pair* ε_{avg}	*HF orbital pair* ε_{avg}	*INDO orbital pair* ε_{avg}
A_{1u}	<5	6*	13*
	H-8, H-9	H, H-1	H, H-1
	−5.16	−6.05	−6.35
A_{2u}	–	<5	7
		H-2, H-3	H-2, H-3
		−6.24	−6.70
d_1 E_g	1360*	850	1692
	H, H-3	H-4, H-7	H-4, H-7
	−4.7	−7.44	−6.93
d_2 E_g	29	5	5
	H-1, H-2	H-5, H-6	H-5, H-6
	−4.7	−7.46	−6.91

† See table 2 for definitions. In this case, the d_1 E_g orbitals have the proper symmetry to interact with the pz π orbitals, while the d_2 E_g orbitals are orthogonal to the pz π orbitals. In the DFT case the A_{2u} orbital pair did not occur in the top ten orbitals of the complex and we thus do not report results for it here. The alternative orbitals that did appear within the highest ten had couplings on the order of 20–40 cm^{-1}.

Table 5. Coupling elements for the Creutz–Taube ion†.

Orbital	*DFT orbital pair* ε_{avg}	*HF orbital pair* ε_{avg}
d_1 E_g	2384*	2064*
	H, H-5	H, H-3
	−16.7	−21.3
d_2 E_g	156	120
	H-3, H-4	H-4, H-5
	−16.8	−21.6
d_3	<5	<5
	H-1, H-2	H-1, H-2
	−16.7	−21.5

† See table 2 for definitions.

significantly smaller than that for the d_1 E_g pair of orbitals.

In order to assess the sensitivity of these results to basis set effects we repeated the coupling element calculations for the bis-CO linear dimer at the B3LYP/DZ D_{2h} geometry using the 3-21G and 3-21+G (diffuse functions on C, N and O) basis sets. While the 3-21G basis set is relatively modest these calculations nevertheless allow us to address the impact of diffuse functions on the coupling. We obtained coupling elements for the two basis sets of (3-21G/3-21+G, in cm^{-1}): $A_{1u} = 35/27$; $A_{2u} = -6/3$ (a—sign indicates the orbitals are inverted compared to the results of table 3); $d_1E_g = 317/270$; and $d_2E_g = 1/13$. The results are in reasonable agreement with each other and with the DZ results, suggesting that further addition of diffuse functions would not alter the conclusions drawn below.

In table 4 we present results for the analogous orbitals of the bis-py complex. We once again find only one large coupling element, and it is again between the d_1 orbitals on each center. In the DFT case one member of this orbital pair correlates with the HOMO of the complex, whereas in the HF and INDO cases the HOMO exhibits weak coupling. However, the HF or INDO results indicate that the orbitals exhibiting large coupling are considerably closer energetically to the HOMO than they were in the bis-CO case. We also performed a B3LYP optimization of this structure in full D_{2h} symmetry using the 3–21G basis. The coupling elements obtained (in cm^{-1}) were: $A_{1u} = 8$; $d_1E_g = 1258$; and $d_2E_g = 62$. While modest differences are found between the results from the two structures and two basis sets it is clear that the overall trends and relative sizes are insensitive to the differences in the calculations.

Table 5 contains results for the Creutz–Taube ion. In this case we focus on the six MOs of the Creutz–Taube ion correlating with the three highest-lying single-center MOs, all of which are principally d-centered. We denote the orbitals in correspondence to the metal Por orbitals, thus the E_g pair is largely the pair of metal d orbitals of d_{yz} and d_{xz} character (where the pz plane is in the *xz* plane) and the third single center orbital (d_3) is primarily d_{xy} in character. The value for the coupling between the d_1 orbitals is larger than that observed for the bis-py complex for this orbital pair, while the remaining coupling elements are considerably smaller. Note that the large coupling element for each method occurs for orbital pairs that include the HOMO. We do not report INDO couplings, but calculations at a similar geometry where all three methods were compared produced results with comparable magnitudes and similar trends to the DFT and HF results at that geometry.

4. Discussion

For calibration purposes we first consider the results for the Creutz–Taube ion. The geometry is similar to that obtained previously by Reimers *et al.* [55] using the same basis except that, since their optimisation was based on the +5 ion whereas we considered the closed-shell +4 ion, we find that the Ru-pz bond length is about 0.1 Å shorter than either of their gas-phase values, but still a good deal larger than the crystallographic value for the +5 ion (1.991 Å). All of the remaining Ru–N bond lengths are approximately 0.1 Å larger than the crystallographic values (2.11–2.12 Å). Bencini *et al.* [56] have examined functional and basis set effects on the geometry of the Creutz–Taube ion and showed that the principal factor affecting the Ru–N geometries is the choice of Ru basis. Inclusion of solvent is also likely to shorten the bond lengths in the ion. For purposes of comparison with our Ru-Por dimer calculations we present results in the same basis used to treat these larger systems.

Our results for the coupling element in the Creutz–Taube ion suggest that a large coupling element is found only for one pair of orbitals in the complex, that being the d_π orbitals that have significant overlap with the π and $\pi*$ orbitals of the intervening pz ligand (i.e. the d_1 orbitals). Our value of 2384 cm^{-1} for the B3LYP results (2064 cm^{-1} for HF) is similar in size to the results of Reimers *et al.* [55] (2400 cm^{-1}) and that inferred from the work of Bencini *et al.* (3092 cm^{-1}) by Reimers *et al.* [55]. These values are also in the general range of what one would infer from experiment on this system [55]. Our value is actually considerably larger than that quoted by Reimers *et al.* [55] for their gas-phase calculations in this basis(1450 cm^{-1}). The difference is likely due to our shorter Ru–N_{pz} bond length. Using a geometry we obtained in a somewhat different basis that gave Ru–N bond lengths similar to those quoted in table 1 except for the Ru–N_{pz} bond length, which was about 0.1 Å longer, we obtained a B3LYP value of the coupling of 1625 cm^{-1}. This emphasizes the geometry sensitivity of the coupling for the Creutz–Taube ion, even with respect to symmetric modes [55]. The coupling obtained for the two remaining occupied d orbitals is considerably smaller that that for the d_1 orbital, falling to on the order of 100 cm^{-1} for the d_2 orbital, and <5 cm^{-1} for the d_3 orbital, again consistent with previous results [55]. From this analysis we conclude that the methods used to treat the Por dimers will give trends consistent with results that would be obtained using more extensive basis sets, and that the relative sizes of couplings for various orbitals should also be reproduced reasonably well.

Two of the three Ru-Por dimers considered here have pz linkages connecting the ruthenium atoms, and each of these exhibits a pair of orbitals (d_1) that has a relatively large coupling element. For the bis-py complex the value is within 40–50% of that for the Creutz–Taube ion, while for the bis-CO case the coupling element (while still large compared to that for the other orbitals of the complex) is only about 10–20% of that for Creutz–Taube ion. We attribute the lowering of the coupling involving the d_1 orbitals in either of the Ru-Por dimers when compared to that found in the Creutz–Taube ion to: (1) greater delocalization of the d_1 type orbital onto the Por (leading to less density on the metal for direct delocalization onto the pz); and (2) considerable π-backbonding of the metal orbitals in the bis-CO case (moving density away from the pz linker). For the other metal orbital (d_2) the coupling is expected to be weak as was found in the Creutz–Taube ion, since its largest overlap occurs with σ orbitals of the pz, which are considerably farther from the metal d orbitals energetically. The other high-lying orbitals (Por-centered) have zero overlap with the pz π orbitals, and are weakly coupled as well.

On the other hand, in the lower symmetry case of the cofacial Por dimer, the couplings between all four high lying monomer orbitals are of comparable size, in the range of several 100 wave-numbers. It should be noted that while the Ru–Ru distance is on the order of 6.5 Å, the ring planes are considerably closer than this (<3.5 Å), leading to relatively large, direct coupling between the rings. In fact, orbital plots suggest considerable direct overlap in these cases, with little to no density on the linking py ligands. In order to check this we considered a modified cofacial dimer, beginning with the geometry used in the calculations quoted in table 2. We then replaced the py linkers with H atoms (at normal C–H bond lengths on their, respective, Por) and calculated the Kohn–Sham orbitals and energies using the B3LYP functional. In this case, no direct bonded pathway exists between the two Por, but we obtained values of the coupling (in cm^{-1}) of A_{1u}: 400.5; A_{2u}: 398.3; d_1E_g: 497.1; and d_2E_g: 265.6. While there are modest differences between the couplings for given orbital pairs with and without the linking py, the results are overall quite similar suggesting that the coupling is largely direct (through space) between the two rings.

Even though each complex possesses an orbital pair with large couplings, this does not mean that rapid electron transfer would be observed in these compounds, or that they would be necessarily Class III compounds, as is believed to be the case for the Creutz–Taube ion [55,80]. This is because, unlike the Creutz–Taube ion where the ligand orbitals are relatively low-energy, the Por ligand has high-lying orbitals. Depending on the nature of the external ligands it may be possible to adjust the relative positions of the metal and Por orbitals, leading to a HOMO with little to no metal character. One notes that the calculated relative orbital energies of the metal-like and Por-based orbitals are considerably closer in the bis-py complex than in the bis-CO complex. In the case of the bis-py complex DFT predicts that the HOMO has strong metal character (similar to the Creutz–Taube ion), whereas all three methods predict that the HOMO in the bis-CO complex is Por-like. Using a geometry obtained for the bis-CO complex having full D_{2h} symmetry (B3LYP/DZ optimization) we were able to use B3LYP ΔSCF calculations in order to obtain many-electron estimates of the relative ionization potentials of the complex. While we were able to converge only six of the eight possible ion states, we found good agreement with the KS orbital ordering and coupling elements where comparisons could be made (coupling elements for the A_{2u} pair and the d_2 E_g pairs) and further found that the lowest-lying ion state indeed involved removal of an electron from an orbital that was principally Por-based.

A difference in character of the HOMO of Ru-Por compounds related to changes in axial ligation has been observed in previous experimental studies [60,81], and is consistent with the trends seen above. In fact, experimental studies of CO Ru-Por monomers indicate

(based on electrochemical and ESR evidence) that ionization yields a Por-localized hole. On the other hand, the analogous bis-py Ru-Por complex is considerably easier to ionize and exhibits properties consistent with metal ionization [60,81]. Ru-Por monomers possessing both py and CO axial ligands are found to behave much like the CO analogues [60]. These results support the trends we observe and when combined with our coupling element calculations suggest that while a compound might have large coupling between a pair of orbitals, the energetic placement of this orbital pair will also be an important factor in determining the actual coupling in the ion. In particular, while strong coupling might be present between an orbital pair, it could be that the electron removed from the neutral species to create the cation might come from an orbital that is largely Por-based (A_{1u} or A_{2u}), yielding low coupling.

This energy-dependent ordering suggests a potential means for controlling the coupling between components in a structure of this type via the nature of the ligands bound to the central metals. It is clear that CO, independent of method, lowers the metal d orbitals relative to the Por orbitals. One could imagine a system tuned such that without CO bound, the HOMO had $d_1$character, but with CO bound, the d_1 orbital is lowered, the Por π orbitals are higher energy, and the coupling is reduced significantly. Such ligand-based switching would be dependent on tuning the metal and Por to yield near-degeneracy, but it is not outside the realm of susbstituent effects that have been previously observed.

Another important result is the general agreement between the three methods used to compute the coupling. Any of the three methods make similar predictions for the number of large or small coupling elements one should expect. In most cases the large coupling elements are within a factor of two of each other for the various methods, and are frequently closer than this. On closer inspection modest differences emerge. The coupling element involving the d_1 orbital pair is predicted to be larger by DFT than HF in the two linear dimers and in the Creutz–Taube ion, while HF produces a somewhat larger coupling element for the d_1 orbital pair in the cofacial case. In the linear dimers and the Creutz–Taube ion the coupling is predominantly mediated by the metal orbital overlap with the pz π and $\pi*$ orbitals, whereas in the cofacial dimer we have shown that direct orbital overlap is the predominant coupling mode. It is possible then that the differences between the two methods arise from modest but important variations in the amount of metal and Por character in the d_1E_g orbital, with greater metal character favoring larger coupling in the linear dimers. Nevertheless, the two methods are always within a factor of two of each other for the large couplings, and within $30\,cm^{-1}$ of each other for smaller couplings. In the linear dimers the INDO results tend to be larger than either the DFT or HF $d_1$orbital couplings, with the smaller couplings again quite close to either the DFT or HF results. In the cofacial dimer there is generally more variability in the INDO results. Again, however, the results are within a factor of two of the DFT or HF results in most cases, and this level of agreement is consistent with results from previous studies when comparing *ab initio* and INDO results [31].

Given the difficulty TDDFT has faced with descriptions of charge transfer transitions [82] it may be surprising that the coupling elements obtained using DFT here are in such good agreement with those obtained by INDO or HF. A previous study has also shown that long-range coupling tends to be overestimated using DFT, due to the underestimation of band gaps [83]. It is believed that these two problems stem from inaccurate calculation of relative KS orbital energies when little overlap exists between the initial and final states [82] and inaccurate band-gaps in extended systems [84,85]. The results presented here indicate that if such effects are present in our systems they are modest. We are presently examining the utility of DFT in model systems that include through-space and through bond coupling in a variety of orientations in order to examine the limits of its usefulness for the study of the electronic coupling element.

5. Future directions

The strides made in recent years in the theoretical treatment of electron transfer processes have been impressive. A variety of methods have appeared that provide access to the electronic coupling element for ground and excited state transfers [66–70,86,87], allow detailed investigation of the dominant pathways for tunnelling [88], and detailed study of energetic effects [1,89]. In addition, strides made in ground state electronic structure theory techniques have allowed electron transfer theorists to estimate inner sphere reorganization energies with considerable accuracy [55]. Finally, the implementation of self-consistent reaction field techniques coupled to accurate quantum chemical methods has yielded considerably more accurate (albeit still dielectric continuum-based) estimates of outer-sphere reorganization energies than have been previously available [90–94]. In some sense, it would seem that the electron transfer theorist has reached "the promised land" and that all one needs to do at present is calculate.

In a qualitative sense this is true, but in another sense electron transfer now must await further refinements/improvements in electronic structure theory to achieve all the goals it has set for itself. The above results indicate that while quantum chemistry methods give similar results with respect to the relative sizes of the couplings in these systems, they have a much more

difficult time agreeing on the relative energies of the various states. This would not be problematic in itself if any one method could be trusted to give uniformly accurate results for the relative energies, but this is clearly not the case. Furthermore, it is not merely ordering the low-lying states of the system that is at issue. Within a superexhchange perspective [12,95], it is the relative energies of all states of the system that is at stake. In many cases the strength of the coupling can be shown to depend weakly on energy gaps [96] but where gaps get small errors in their separation can lead to wide variations and potential errors in the computed coupling [52]. The solution might at first glance appear to be DFT based on a (near-) exact functional (a non-trivial task to be sure), but we are still at a stage where the meaning of the KS-orbital energies is an open question. In addition, this would still not mean that excited states would necessarily be treated accurately in a TDDFT-type formalism.

In many respects, short of full-CI type results which will perennially be out of the question for charge-transfer systems of interest to experimentalists, the equations of motion coupled cluster approach (e.g. EOM-CCSD)[97] method would appear to be a powerful *ab initio* technique to generate ground and excited states of relevance to electron transfer. The method combines high-accuracy with at least some measure of scalability. It has been used previously to treat small model systems [29,30]. Nevertheless, it too will be limited in the near future to systems containing tens, not hundreds of atoms. Larger systems could in principle be treated using the similarity-transformed equations of motion coupled cluster approach of Nooijen and Bartlett [98], but this method also requires a correlated ground state that will limit its applicability to well under 50 atom systems.

Obviously, there is still much to learn from more approximate calculations. Recent results indicate that while approximate methods may miss details of the electronic structure, the electronic coupling tends to be relatively insensitive to correlation effects except where near-degeneracies are an issue [29,30]. This suggests that accurate results for many important reactions are accessible via uncorrelated (HF) or semi-empirical approaches.

The second area that will require significant attention is the treatment of the wide range of nuclear geometries from which electron transfer reactions can occur in real systems. The majority of previous studies of the electronic coupling element have focused on a single geometry or a few idealized nuclear geometries. This may be appropriate in rigid systems, but in bimolecular reactions [24] (where many possible orientations are possible) or in systems that are flexible (e.g biological systems) thermal fluctuations [52,99], may lead to significant modifications in the coupling. A number of groups have attempted to address these issues by combining MD with quantum mechanical calculations of the coupling element [24,31,52,99]. These results reinforce the idea that large variations in the coupling should be expected in cases where thermal fluctuations can modify orientations and/or charge transfer distances.

Recent results suggest the additional issue of non-Condon effects brought about by nuclear motions will not be a problem in most cases [100], but there still is the question of thermal averaging. In addition, as some authors have suggested, there is the possibility of gating conformations playing a dominant role in the rate of the reaction [101]. These conformations correspond to nuclear configurations that are not connected to the reorganization associated with the electron transfer but nevertheless are important because they correspond to geometries of particularly high coupling elements. While they may not be low-energy, they can be important in long-distance transfers because of the larger coupling and enhanced rates. The location of such gating conformations, if they exist, is a serious question in itself, but the further assessment of their relative importance will require high accuracy from whatever structural models (molecular mechanics, semi-empirical or *ab initio* quantum mechanics) are used to describe the system.

All of which suggests that, far from being a nearly-completed journey, the development of new theoretical and new computational methods in electron transfer are as important as ever before, making theoretical electron transfer a continually evolving and exciting discipline in which to work.

6. Conclusions

We presented results for the electronic coupling element for electron transfer for three Ru-Por dimers. Using orbital energy differences based on DFT/B3LYP, RHF, and INDO results we compared coupling elements between the compounds for several orbital pairs. The results suggest that all three methods give qualitatively similar values of the coupling at a given geometry and that the coupling involving the highest occupied molecular orbital can be changed markedly by changes in orientation or by changes in the external axial ligand. We are currently investigating the coupling in asymmetric dimers and exploring geometrical effects on the size of the coupling.

Acknowledgements

We wish to acknowledge financial support from the National Science Foundation (CHE-9731634, CHE-0353199), and the Donors of the Petroleum Research Fund.

Appendix 1. Geometries.

Cofacial dimer					
1	6	0	1.356470	1.121171	−3.512404
2	6	0	−1.356470	−1.121171	−3.512404
3	6	0	1.828850	0.261501	−2.551370
4	6	0	−1.828850	−0.261501	−2.551370
5	6	0	1.400777	0.781302	−1.254501
6	6	0	−1.400777	−0.781302	−1.254501
7	7	0	0.674055	1.946360	−1.459691
8	7	0	−0.674055	−1.946360	−1.459691
9	6	0	0.634062	2.184654	−2.826603
10	6	0	−0.634062	−2.184654	−2.826603
11	6	0	−1.121573	5.553577	−3.516624
12	6	0	1.121573	−5.553577	−3.516624
13	6	0	−1.540563	6.436998	−2.545867
14	6	0	1.540563	−6.436998	−2.545867
15	6	0	−1.267670	5.820072	−1.253672
16	6	0	1.267670	−5.820072	−1.253672
17	7	0	−0.703682	4.566222	−1.464334
18	7	0	0.703682	−4.566222	−1.464334
19	6	0	−0.579805	4.384967	−2.833346
20	6	0	0.579805	−4.384967	−2.833346
21	6	0	1.830884	0.260725	2.549661
22	6	0	−1.830884	−0.260725	2.549661
23	6	0	1.359757	1.119947	3.511619
24	6	0	−1.359757	−1.119947	3.511619
25	6	0	0.636895	2.183955	2.827137
26	6	0	−0.636895	−2.183955	2.827137
27	7	0	0.674978	1.946640	1.460039
28	7	0	−0.674978	−1.946640	1.460039
29	6	0	1.401507	0.781318	1.253623
30	6	0	−1.401507	−0.781318	1.253623
31	6	0	−1.116108	5.552811	3.520245
32	6	0	1.116108	−5.552811	3.520245
33	6	0	−1.536321	6.436165	2.550045
34	6	0	1.536321	−6.436165	2.550045
35	6	0	−1.265161	5.819150	1.257523
36	6	0	1.265161	−5.819150	1.257523
37	7	0	−0.700487	4.565170	1.467405
38	7	0	0.700487	−4.565170	1.467405
39	6	0	−0.575338	4.384225	2.836221
40	6	0	0.575338	−4.384225	2.836221
41	6	0	0.036129	3.283293	3.455882
42	6	0	−0.036129	−3.283293	3.455882
43	6	0	−1.521902	6.395243	0.002400
44	6	0	1.521902	−6.395243	0.002400
45	6	0	0.031690	3.284281	−3.453683
46	6	0	−0.031690	−3.284281	−3.453683
47	6	0	1.717040	0.218590	−0.000572
48	6	0	−1.717040	−0.218590	−0.000572
49	1	0	1.476618	1.050145	−4.585494
50	1	0	−1.476618	−1.050145	−4.585494
51	1	0	2.397182	−0.645635	−2.699226
52	1	0	−2.397182	0.645635	−2.699226
53	1	0	−1.158161	5.678432	−4.591155
54	1	0	1.158161	−5.678432	−4.591155
55	1	0	−1.983087	7.415445	−2.681232
56	1	0	1.983087	−7.415445	−2.681232
57	1	0	2.399465	−0.646439	2.696319
58	1	0	−2.399465	0.646439	2.696319
59	1	0	1.480649	1.048284	4.584586
60	1	0	−1.480649	−1.048284	4.584586
61	1	0	−1.150989	5.677615	4.594827
62	1	0	1.150989	−5.677615	4.594827
63	1	0	−1.978910	7.414526	2.685872
64	1	0	1.978910	−7.414526	2.685872
65	1	0	0.085548	3.304654	4.542005
66	1	0	−0.085548	−3.304654	4.542005
67	1	0	−1.956779	7.391555	0.003321
68	1	0	1.956779	−7.391555	0.003321
69	1	0	0.079731	3.306246	−4.539882
70	1	0	−0.079731	−3.306246	−4.539882
71	44	0	0.000000	3.258984	−0.000564
72	44	0	0.000000	−3.258984	−0.000564
73	6	0	4.032415	−0.651195	−0.002395

Appendix 1 – *continued*

74	6	0	−4.032415	0.651195	−0.002395
75	1	0	4.324686	0.393660	−0.002680
76	1	0	−4.324686	−0.393660	−0.002680
77	6	0	4.992834	−1.670579	−0.003371
78	6	0	−4.992834	1.670579	−0.003371
79	1	0	6.053445	−1.434526	−0.004385
80	1	0	−6.053445	1.434526	−0.004385
81	6	0	4.539754	−2.999351	−0.003081
82	6	0	−4.539754	2.999351	−0.003081
83	1	0	5.227252	−3.839075	−0.003897
84	1	0	−5.227252	3.839075	−0.003897
85	6	0	3.160847	−3.240264	−0.001705
86	6	0	−3.160847	3.240264	−0.001705
87	1	0	2.799308	−4.254446	−0.001480
88	1	0	−2.799308	4.254446	−0.001480
89	7	0	2.211392	−2.257473	−0.000611
90	7	0	−2.211392	2.257473	−0.000611
91	6	0	2.651740	−0.959577	−0.001040
92	6	0	−2.651740	0.959577	−0.001040
93	6	0	1.627161	4.112608	−0.001145
94	6	0	−1.627161	−4.112608	−0.001145
95	8	0	2.678942	4.659850	−0.001277
96	8	0	−2.678942	−4.659850	−0.001277
Bis-CO dimer					
1	6	0	−3.522111	2.549152	3.580821
2	6	0	−3.522187	2.549046	−3.580834
3	6	0	−2.545637	3.519692	3.544687
4	6	0	−2.545743	3.519616	−3.544690
5	6	0	−1.256139	2.837505	3.528107
6	6	0	−1.256224	2.837467	−3.528106
7	7	0	−1.474070	1.467224	3.546790
8	7	0	−1.474115	1.467180	−3.546788
9	6	0	−2.846783	1.256182	3.583081
10	6	0	−2.846820	1.256097	−3.583089
11	6	0	−3.522362	−2.548773	3.580855
12	6	0	−3.522284	−2.548879	−3.580874
13	6	0	−2.546014	−3.519440	3.544712
14	6	0	−2.545908	−3.519517	−3.544707
15	6	0	−1.256412	−2.837369	3.528120
16	6	0	−1.256327	−2.837407	−3.528119
17	7	0	−1.474238	−1.467057	3.546797
18	7	0	−1.474194	−1.467102	−3.546795
19	6	0	−2.846918	−1.255910	3.583094
20	6	0	−2.846880	−1.255995	−3.583102
21	6	0	2.546014	3.519440	3.544712
22	6	0	2.545908	3.519517	−3.544707
23	6	0	3.522362	2.548773	3.580855
24	6	0	3.522284	2.548879	−3.580874
25	6	0	2.846918	1.255910	3.583094
26	6	0	2.846880	1.255995	−3.583102
27	7	0	1.474238	1.467057	3.546797
28	7	0	1.474194	1.467102	−3.546795
29	6	0	1.256412	2.837369	3.528120
30	6	0	1.256327	2.837407	−3.528119
31	6	0	3.522111	−2.549152	3.580821
32	6	0	3.522187	−2.549046	−3.580834
33	6	0	2.545637	−3.519692	3.544687
34	6	0	2.545743	−3.519616	−3.544690
35	6	0	1.256139	−2.837505	3.528107
36	6	0	1.256224	−2.837467	−3.528106
37	7	0	1.474070	−1.467224	3.546790
38	7	0	1.474115	−1.467180	−3.546788
39	6	0	2.846783	−1.256182	3.583081
40	6	0	2.846820	−1.256097	−3.583089
41	6	0	3.475721	−0.000193	3.605684
42	6	0	3.475720	−0.000088	−3.605697
43	6	0	−0.000192	−3.463766	3.512162
44	6	0	−0.000088	−3.463767	−3.512160
45	6	0	−3.475721	0.000193	3.605684
46	6	0	−3.475720	0.000088	−3.605697
47	6	0	0.000192	3.463766	3.512162
48	6	0	0.000088	3.463767	−3.512160
49	1	0	−4.595640	2.684354	3.605392
50	1	0	−4.595720	2.684215	−3.605414

Appendix 1 – *continued*

51	1	0	−2.674767	4.594221	3.534104
52	1	0	−2.674906	4.594141	−3.534107
53	1	0	−4.595914	−2.683891	3.605442
54	1	0	−4.595832	−2.684030	−3.605475
55	1	0	−2.675226	−4.593947	3.534138
56	1	0	−2.675088	−4.594027	−3.534128
57	1	0	2.675226	4.593947	3.534138
58	1	0	2.675088	4.594027	−3.534128
59	1	0	4.595914	2.683891	3.605442
60	1	0	4.595832	2.684030	−3.605475
61	1	0	4.595640	−2.684354	3.605392
62	1	0	4.595720	−2.684215	−3.605414
63	1	0	2.674767	−4.594221	3.534104
64	1	0	2.674906	−4.594141	−3.534107
65	1	0	4.562289	−0.000208	3.640742
66	1	0	4.562288	−0.000070	−3.640764
67	1	0	−0.000209	−4.551089	3.501006
68	1	0	−0.000072	−4.551089	−3.501004
69	1	0	−4.562289	0.000208	3.640742
70	1	0	−4.562288	0.000070	−3.640764
71	44	0	0.000000	0.000000	3.608491
72	44	0	0.000000	0.000000	−3.608484
73	6	0	−1.160079	−0.000008	0.700434
74	7	0	0.000000	0.000000	1.408464
75	6	0	1.160079	0.000008	0.700434
76	6	0	1.160080	0.000009	−0.700417
77	1	0	2.085921	0.000016	−1.257488
78	7	0	0.000000	0.000000	−1.408452
79	6	0	−1.160080	−0.000009	−0.700417
80	1	0	−2.085921	−0.000016	−1.257488
81	6	0	0.000000	0.000000	5.476357
82	6	0	0.000000	0.000000	−5.476348
83	8	0	0.000000	0.000000	6.658853
84	8	0	0.000000	0.000000	−6.658843
85	1	0	2.085921	0.000015	1.257493
86	1	0	−2.085921	−0.000015	1.257493
87	1	0	0.000209	4.551089	3.501006
88	1	0	0.000072	4.551089	−3.501004
Bis-pyridine dimer					
1	6	0	2.547040	3.517958	3.544148
2	6	0	2.547040	3.517958	−3.544148
3	6	0	3.519390	2.544648	3.483192
4	6	0	3.519390	2.544648	−3.483192
5	6	0	2.839517	1.254067	3.467440
6	6	0	2.839517	1.254067	−3.467440
7	7	0	1.464353	1.463700	3.513940
8	7	0	1.464353	1.463700	−3.513940
9	6	0	1.255932	2.839105	3.559756
10	6	0	1.255932	2.839105	−3.559756
11	6	0	−2.544611	3.519718	3.544129
12	6	0	−2.544611	3.519718	−3.544129
13	6	0	−3.517638	2.547083	3.483157
14	6	0	−3.517638	2.547083	−3.483157
15	6	0	−2.838667	1.256031	3.467399
16	6	0	−2.838667	1.256031	−3.467399
17	7	0	−1.463358	1.464706	3.513982
18	7	0	−1.463358	1.464706	−3.513982
19	6	0	−1.253979	2.839965	3.559740
20	6	0	−1.253979	2.839965	−3.559740
21	6	0	3.517623	−2.547080	3.483108
22	6	0	3.517623	−2.547080	−3.483108
23	6	0	2.544595	−3.519716	3.544054
24	6	0	2.544595	−3.519716	−3.544054
25	6	0	1.253964	−2.839963	3.559707
26	6	0	1.253964	−2.839963	−3.559707
27	7	0	1.463341	−1.464704	3.513927
28	7	0	1.463341	−1.464704	−3.513927
29	6	0	2.838652	−1.256027	3.467395
30	6	0	2.838652	−1.256027	−3.467395
31	6	0	−2.547055	−3.517951	3.544201
32	6	0	−2.547055	−3.517951	−3.544201
33	6	0	−3.519405	−2.544642	3.483225
34	6	0	−3.519405	−2.544642	−3.483225
35	6	0	−2.839533	−1.254062	3.467439

Appendix 1 – *continued*

36	6	0	−2.839533	−1.254062	−3.467439
37	7	0	−1.464368	−1.463694	3.513992
38	7	0	−1.464368	−1.463694	−3.513992
39	6	0	−1.255946	−2.839100	3.559775
40	6	0	−1.255946	−2.839100	−3.559775
41	6	0	−0.001206	−3.468088	3.592233
42	6	0	−0.001206	−3.468088	−3.592233
43	6	0	−3.467541	0.001201	3.434065
44	6	0	−3.467541	0.001201	−3.434065
45	6	0	0.001192	3.468092	3.592245
46	6	0	0.001192	3.468092	−3.592245
47	6	0	3.467526	−0.001197	3.434089
48	6	0	3.467526	−0.001197	−3.434089
49	1	0	2.679566	4.592059	3.571572
50	1	0	2.679566	4.592059	−3.571572
51	1	0	4.593463	2.676382	3.450858
52	1	0	4.593463	2.676382	−3.450858
53	1	0	−2.676397	4.593902	3.571568
54	1	0	−2.676397	4.593902	−3.571568
55	1	0	−4.591628	2.679564	3.450826
56	1	0	−4.591628	2.679564	−3.450826
57	1	0	4.591612	−2.679560	3.450758
58	1	0	4.591612	−2.679560	−3.450758
59	1	0	2.676382	−4.593901	3.571454
60	1	0	2.676382	−4.593901	−3.571454
61	1	0	−2.679581	−4.592051	3.571647
62	1	0	−2.679581	−4.592051	−3.571647
63	1	0	−4.593478	−2.676376	3.450899
64	1	0	−4.593478	−2.676376	−3.450899
65	1	0	−0.001576	−4.554971	3.628798
66	1	0	−0.001576	−4.554971	−3.628798
67	1	0	−4.554302	0.001561	3.393654
68	1	0	−4.554302	0.001561	−3.393654
69	1	0	0.001561	4.554974	3.628818
70	1	0	0.001561	4.554974	−3.628818
71	44	0	−0.000006	0.000003	3.510060
72	44	0	−0.000006	0.000003	−3.510060
73	6	0	0.000191	1.159636	0.697540
74	7	0	−0.000041	0.000001	1.420924
75	6	0	−0.000252	−1.159635	0.697541
76	6	0	−0.000252	−1.159635	−0.697541
77	1	0	−0.000398	−2.088718	−1.248034
78	7	0	−0.000041	0.000001	−1.420924
79	6	0	0.000191	1.159636	−0.697540
80	1	0	0.000381	2.088720	−1.248030
81	1	0	−0.000398	−2.088718	1.248034
82	1	0	0.000381	2.088720	1.248030
83	1	0	4.554288	−0.001557	3.393678
84	1	0	4.554288	−0.001557	−3.393678
85	7	0	0.000028	−0.000006	5.635029
86	7	0	0.000028	−0.000006	−5.635029
87	6	0	−1.170440	0.000118	6.335732
88	6	0	−1.170440	0.000118	−6.335732
89	6	0	−1.207276	0.000112	7.736742
90	6	0	−1.207276	0.000112	−7.736742
91	6	0	0.000073	−0.000019	8.458431
92	6	0	0.000073	−0.000019	−8.458431
93	6	0	1.207400	−0.000142	7.736703
94	6	0	1.207400	−0.000142	−7.736703
95	6	0	1.170517	−0.000135	6.335695
96	6	0	1.170517	−0.000135	−6.335695
97	1	0	−2.080458	0.000214	5.752521
98	1	0	−2.080458	0.000214	−5.752521
99	1	0	−2.167948	0.000210	8.242380
100	1	0	−2.167948	0.000210	−8.242380
101	1	0	0.000093	−0.000025	9.545027
102	1	0	0.000093	−0.000025	−9.545027
103	1	0	2.168087	−0.000247	8.242313
104	1	0	2.168087	−0.000247	−8.242313
105	1	0	2.080515	−0.000227	5.752446
106	1	0	2.080515	−0.000227	−5.752446
Creutz–taube ion					
1	6	0	0.001386	0.699275	1.160872
2	6	0	−0.001386	−0.699275	1.160872

Appendix 1 – *continued*

3	7	0	0.000141	−1.456420	0.005617
4	6	0	0.001386	−0.699304	−1.149383
5	6	0	−0.001386	0.699304	−1.149383
6	7	0	−0.000141	1.456420	0.005617
7	1	0	0.004649	1.228256	2.106052
8	1	0	−0.004649	−1.228256	2.106052
9	1	0	0.004118	−1.227774	−2.095182
10	1	0	−0.004118	1.227774	−2.095182
11	44	0	0.000389	3.573208	−0.000014
12	44	0	−0.000389	−3.573208	−0.000014
13	7	0	1.652533	3.652371	1.462738
14	1	0	2.156172	2.760205	1.524107
15	1	0	1.343675	3.893432	2.412439
16	1	0	2.346389	4.363507	1.200163
17	7	0	1.506537	3.626036	−1.615797
18	1	0	1.991671	2.727486	−1.718658
19	1	0	1.109676	3.865734	−2.532669
20	1	0	2.234061	4.326677	−1.425598
21	7	0	0.000141	5.789382	−0.008704
22	1	0	0.697451	6.182834	−0.653061
23	1	0	−0.903928	6.182321	−0.299501
24	1	0	0.203399	6.183722	0.918328
25	7	0	−1.650486	3.636584	−1.464920
26	1	0	−1.385883	4.115049	−2.334965
27	1	0	−1.984843	2.700882	−1.721898
28	1	0	−2.464346	4.142356	−1.093629
29	7	0	−1.503646	3.657229	1.616351
30	1	0	−2.093110	4.494507	1.528458
31	1	0	−2.134739	2.848036	1.592389
32	1	0	−1.095019	3.697164	2.557899
33	7	0	−1.506537	−3.626036	−1.615797
34	1	0	−1.109676	−3.865734	−2.532669
35	1	0	−1.991671	−2.727486	−1.718658
36	1	0	−2.234061	−4.326677	−1.425598
37	7	0	−1.652533	−3.652371	1.462738
38	1	0	−2.346389	−4.363507	1.200163
39	1	0	−1.343675	−3.893432	2.412439
40	1	0	−2.156172	−2.760205	1.524107
41	7	0	−0.000141	−5.789382	−0.008704
42	1	0	0.903928	−6.182321	−0.299501
43	1	0	−0.203399	−6.183722	0.918328
44	1	0	−0.697451	−6.182834	−0.653061
45	7	0	1.503646	−3.657229	1.616351
46	1	0	2.134739	−2.848036	1.592389
47	1	0	1.095019	−3.697164	2.557899
48	1	0	2.093110	−4.494507	1.528458
49	7	0	1.650486	−3.636584	−1.464920
50	1	0	2.464346	−4.142356	−1.093629
51	1	0	1.385883	−4.115049	−2.334965
52	1	0	1.984843	−2.700882	−1.721898

References

[1] S.S. Skourtis, D.N. Beratan. Theories of structure-function relationships for bridge-mediated electron transfer reactions. *Electron Transfer-from Isolated Molecules to Biomolecules*, Pt 1, pp. 377–452 (1999).

[2] M.D. Newton, R.J. Cave. Molecular control of electorn and hole transfer processes: theory and applications. In *Molecular Electronics*, J. Jortner, M. Ratner (Eds.), Blackwell, Malden, MA (1997).

[3] R.A. Marcus. On the theory of electron transfer reactions VI. Unified treatment for homgeneous and electrode reactions. *J. Chem. Phys.*, **43**, 679 (1965).

[4] N.S. Hush. Adiabtic theory of outer sphere electron transfer reactions in solution. *Trans. Faraday Soc.*, **57**, 557 (1961).

[5] V.G. Levich. Present state of the theory of oxidation–reduction reactions in solution (Bulk and Electrode Reactions). *Adv. Electrochem. Electrochem. Eng.*, **4**, 249 (1966).

[6] R.R. Dogonadze, A.M. Kuznetsov, M.A. Vorotyntsev. On the theory of nonradiative transitions in polar media. *Phys. Status Solidi B*, **54** (1972) 125, 425.

[7] N.R. Kestner, J. Logan, J. Jortner. Thermal electron transfer reactions in polar solvents. *J. Phys. Chem.*, **78**, 2148 (1974).

[8] M. Bixon, J. Jortner. Electron transfer—from isolated molecules to biomolecules. *Electron Transfer-from Isolated Molecules to Biomolecules*, Pt 1, pp. 35–202 (1999).

[9] H. Sumi, R.A. Marcus. Dynamical effects in electron transfer reactions. *J. Chem. Phys.*, **84**, 4894 (1986).

[10] J. Jortner, M. Bixon. Intramolecular vibrational excitations accompanying solvent-controlled electron transfer reactions. *J. Chem. Phys.*, **88**, 167 (1988).

[11] R.A. Marcus, N. Sutin. Electron transfers in chemistry and biology. *Biochim. Biophys. Acta*, **811**, 265 (1985).

[12] M.D. Newton. Quantum chemical probes of electron transfer kinetics. *Chem. Rev.*, **91**, 767 (1991).

[13] M.D. Newton, N. Sutin. Electron transfer reaction in condensed phases. *Annu. Rev. Phys. Chem.*, **35**, 437 (1985).
[14] M.D. Newton. Quantum chemical probes of electron-transfer kinetics—the nature of donor-acceptor interactions. *Chem. Rev.*, **91**, 767 (1991).
[15] D.N. Beratan, J.J. Hopfield. Calculation of electron tunneling matrix elements in rigid systems: mixed-valence dithiospirocuclobutane molecules. *J. Am. Chem. Soc.*, **106**, 1584 (1984).
[16] D.N. Beratan, J.N. Onuchic. Electron-transfer—from model compounds to proteins. *Adv. Chem. Ser.*, 71 (1991).
[17] S. Larsson. Electron-exchange reactions in aqueous solution. *J. Phys. Chem.*, **88**, 1321 (1984).
[18] S. Larsson. Electron transfer in proteins. *Biochim. Biophys. Acta Bioenerg.*, **1365**, 294 (1998).
[19] S. Larsson. Energy saving electron pathways in proteins. *J. Biol. Inorg. Chem.*, **5**, 560 (2000).
[20] S. Larsson, M. Braga. Calculation of the electronic factor. *J. Photochem. Photobiol. A. Chem.*, **82**, 61 (1994).
[21] L.A. Curtiss, C.A. Naleway, J.R. Miller. Theoretical study of long distance coupling in $H_2C(CH_2)n{-}2CH_2$ Chains, $n = 3{-}16$. *J. Phys. Chem.*, **97**, 4050 (1993).
[22] L.A. Curtiss, C.A. Naleway, J.R. Miller. Superexchange pathway calculation of electronic coupling through cyclohexane spacers. *J. Phys. Chem.*, **99**, 1182 (1995).
[23] R.J. Cave, D.V. Baxter, W.A. Goddard, J.D. Baldeschwieler. Theoretical-studies of electron-transfer in metal dimers—Xy + −]X + Y, Where X, Y = Be, Mg, Ca, Zn, Cd. *J. Chem. Phys.*, **87**, 926 (1987).
[24] E.W. Castner, D. Kennedy, R.J. Cave. Solvent as electron donor: donor/acceptor electronic coupling is a dynamical variable. *J. Phys. Chem. A*, **104**, 2869 (2000).
[25] R.J. Cave, S.J. Klippenstein, R.A. Marcus. A Semiclassical model for orientation effects in electron-transfer reactions. *J. Chem. Phys.*, **84**, 3089 (1986).
[26] R.J. Cave, P. Siders, R.A. Marcus. Mutual orientation effects on electron-transfer between porphyrins. *J. Phys. Chem.*, **90**, 1436 (1986).
[27] P.D. Siders, R.J. Cave, R.A. Marcus. A model for orientation effects in electron-transfer reactions. *J. Chem. Phys.*, **81**, 5613 (1984).
[28] D.N. Beratan, J.N. Onuchic, J.J. Hopfield. Electron-tunneling through covalent and noncovalent pathways in proteins. *J. Chem. Phys.*, **86**, 4488 (1987).
[29] E. Cukier, S. Daniels, E. Vinson, R.J. Cave. Are hydrogen bonds unique among weak interactions in their ability to mediate electronic coupling? *J. Phys. Chem. A*, **106**, 11240 (2002).
[30] E. Cukier, R.J. Cave. A comparison of through-space and through-bond coupling for tunneling in alkane chains. *Chem. Phys. Lett.*, **402**, 186 (2005).
[31] N.E. Miller, M.C. Wander, R.J. Cave. A theoretical study of the electronic coupling element for electron transfer in water. *J. Phys. Chem. A*, **103**, 1084 (1999).
[32] M.R. Wasielewski. Photoinduced electron-transfer in supramolecular systems for artificial photosynthesis. *Chem. Rev.*, **92**, 435 (1992).
[33] J.P. Collman, C.E. Barnes, T.J. Collins, P.J. Brothers, J. Gallucci, J.A. Ibers. Binuclear ruthenium(II) porphyrins: reinvestigation of their preparation, characterization, and interactions with molecular oxygen. *J. Am. Chem. Soc.*, 7030 (1981).
[34] D. Gust, T.A. Moore, P.A. Liddell, G.A. Nemeth, L.R. Makings, A.L. Moore, D. Barrett, P.J. Pessiki, R.V. Bensasson, M. Rougee, C. Chachaty, F.C. Deschryver, M. Vanderauweraer, A.R. Holzwarth, J.S. Connolly. Charge separation in carotenoporphyrin—quinone triads—synthetic, conformational, and fluorescence lifetime studies. *J. Am. Chem. Soc.*, **109**, 846 (1987).
[35] D. Gust, T.A. Moore, L.R. Makings, P.A. Liddell, G.A. Nemeth, A.L. Moore. Photodriven electron-transfer in triad molecules—a 2-step charge recombination reaction. *J. Am. Chem. Soc.*, **108**, 8028 (1986).
[36] L.Y. Zhang, R.A. Friesner, R.B. Murphy. *Ab initio* quantum chemical calculation of electron transfer matrix elements for large molecules. *J. Chem. Phys.*, **107**, 450 (1997).
[37] J.P. Collman, J.T. McDevitt, C.R. Leidner, G.T. Yee, J.B. Torrance, W.A. Little. Synthetic, electrochemical, optical, and conductivity studies of coordination polymers of iron, ruthenium, and osmium octaethylporphyrin. *J. Am. Chem. Soc.*, **109**, 4606 (1987).
[38] J.P. Collman, J.T. McDevitt, G.T. Yee, C.R. Leidner, L.G. McCullough, W.A. Little, J.B. Torrance. Conductive polymers derived from iron, ruthenium, and osmium metalloporphyrins: the shish-kebab approach. *Proc. Natl. Acad. Sci. USA*, **83**, 4581 (1986).
[39] H.L. Anderson. Building molecular wires from the colours of life: conjugated porphyrin oligomers. *Chem. Commun. (Camb.)*, 2323 (1999).
[40] N. Aratani, A. Osuka, Y.H. Kim, D.H. Jeong, D. Kim. Extremely long, discrete meso−meso-coupled porphyrin arrays. *Angew. Chem. Int. Ed.*, **39**, 1458 (2000).
[41] L. Baldini, C.A. Hunter. Self-assembly of porphyrin arrays. *Adv. Inorg. Chem.*, 213 (2002).
[42] R.A. Haycock, C.A. Hunter, D.A. James, U. Michelsen, L.R. Sutton. Self-assembly of oligomeric porphyrin rings. *Org. Lett.*, 2435 (2000).
[43] G.A.T. Mines, B.C. Tzeng, K.J. Stevenson, J. Li, J.T. Hupp. Microporous supramolecular coordination compounds as chemosensory photonic lattices. *Angew. Chem.*, **41**, 154 (2002).
[44] K.F.S. Czaplewski, J.T. Hupp, R.Q. Snurr. Molecular squares as molecular sieves: size-selective transport through porous-membrane-supported thin-film materials. *Adv. mater.*, 1895 (2001).
[45] R.T. Kumar, I. Diskin-Posner, I. Goldberg. Solid-state supramolecular chemistry of porphyrins. Ligand-bridged tetraphenylmetalloporphyrin dimers. *J. Inclusion Phenom. Macrocycl. Chem.*, 219 (2000).
[46] N. Aratani, A. Osuka. A new strategy for construction of covalently linked giant porphyrin arrays with one, two, and three dimensionally arranged architectures. *Bull. Chem. Soc. Jpn.*, 1361 (2001).
[47] J.J. Piet, P.N. Taylor, B.R. Wegewijs, H.L. Anderson, A. Osuka, J.M. Warman. Photoexcitations of covalently bridged zinc porphyrin oligomers: Frenkel versus Wannier−Mott type excitons. *J. Phys. Chem. B*, 97 (2001).
[48] T.-B. Tsao, G.-H. Lee, C.-Y. Yeh, S.-M. Peng. Supramolecular assembly of linear trinickel complexes incorporating metalloporphyrins: a novel one-dimensional polymer and oligomer. *Dalton Trans.*, 1465 (2003).
[49] R.S. Loewe, R.K. Lammi, J.R. Diers, C. Kirmaier, D.F. Bocian, D. Holten, J.S. Lindsey. Design and synthesis of light-harvesting rods for intrinsic rectification of the migration of excited-state energy and ground-state holes. *J. Mater. Chem.*, 1530 (2002).
[50] T.S. Balaban, R. Goddard, M. Linke-Schaetzel, J.-M. Lehn. 2-Aminopyrimidine directed self-assembly of zinc porphyrins containing bulky 3,5-Di-tert-butylphenyl groups. *J. Am. Chem. Soc.*, 4233 (2003).
[51] M.L. Merlau, M. del Pilar Mejia, S.T. Nguyen, J.T. Hupp. Artificial enzymes formed via directed assembly of molecular square-encapsulated epoxidation catalysts. *Angew. Chem.*, **40**, 4369 (2001).
[52] T. Kawatsu, D.N. Beratan, T. Kakitani. Conformationally averaged score functions for electronic propagation in proteins. *J. Phys. Chem. B*, **110** (2006) in press.
[53] K. Funatsu, T. Imamura, A. Ichimura, Y. Sasaki. Novel cofacial ruthenium(II) porphyrin dimers and tetramers. *Inorg. Chem.*, **37**, 4986 (1998).
[54] B.S. Brunschwig, C. Creutz, N. Sutin. Electroabsorption spectroscopy of charge transfer states of transition metal complexes. *Coord. Chem. Rev.*, **177**, 61 (1998).
[55] J.R. Reimers, Z.-L. Cai, N.S. Hush. *A priori* evaluation of the solvent contribution to the reorganization energy accompanying intramolecular electron transfer: predicting the nature of the Creutz−Taube ion. *Chem. Phys.*, **319**, 39 (2005).
[56] A. Bencini, I. Ciofini, C.A. Daul, A. Ferretti. Ground and excited state properties and vibronic coupling analysis of the Creutz−Taube ion, $C[(NH_3)(5)Ru\text{-}pyridine\text{-}Ru(NH_3)(5)](5+)$, using DFT. *J. Am. Chem. Soc.*, **121**, 11418 (1999).
[57] A.D. Becke. Density-functional theory thermochemistry. 3. The role of exact exchange. *J. Chem. Phys.*, **98**, 5648 (1993).
[58] P.J. Hay, W.R. Wadt. *Ab initio* effective core potentials for molecular calculations—potentials for the transition metal atoms Sc to Hg. *J. Chem. Phys.*, **82**, 270 (1985).
[59] T.H.J. Dunning, P.J. Hay. Gaussian basis sets for molecular calculations. In *Methods of Electronic Structure Theory*, H.F. Schaefer (Ed.), pp. 1−50, Plenum, New York (1977).
[60] G.M. Brown, F.R. Hopf, T.J. Meyer, D.G. Whitten. Effect of extraplanar ligands on the redox properties and the site of oxidation in iron, ruthenium, and osmium porphyrin complexes. *J. Am. Chem. Soc.*, **97**, 5385 (1975).
[61] C. Liang, M.D. Newton. *Ab Initio* studies of electron transfer: pathway analysis of effective transfer integrals. *J. Phys. Chem.*, **96**, 2855 (1992).

[62] C. Liang, M.D. Newton. *Ab Initio* studies of electron transfer 2. Pathway analysis for homologous organic spacers. *J. Phys. Chem.*, **97**, 3199 (1992).

[63] L.A. Curtiss, J.R. Miller. Distance dependence of electronic coupling through trans alkyl chains: effects of electron correlation. *J. Phys. Chem. A*, **102**, 160 (1998).

[64] C.X. Liang, M.D. Newton. *Ab initio* studies of electron-transfer—pathway analysis of effective transfer integrals. *J. Phys. Chem.*, **96**, 2855 (1992).

[65] J. Logan, M.D. Newton. *Ab Initio* study of electronic coupling in the aqueous Fe + 2–Fe + 3 electron exchange process. *J. Chem. Phys.*, 4086 (1983).

[66] I.V. Kurnikov, D.N. Beratan. *Ab initio* based effective hamiltonians for long-range electron transfer: Hartree–Fock analysis. *J. Chem. Phys.*, **105**, 9561 (1996).

[67] A.A. Stuchebrukhov. Tunneling currents in long-distance electron transfer reactions. III. Many-electron formulation. *J. Chem. Phys.*, **108**, 8499 (1998).

[68] A.A. Stuchebrukhov. Tunneling currents in long-distance electron transfer reactions. IV. Many-electron formulation. Nonorthogonal atomic basis sets and Mulliken population analysis. *J. Chem. Phys.*, **108**, 8510 (1998).

[69] R.J. Cave, M.D. Newton. Generalization of the Mulliken–Hush treatment for the calculation of electron transfer matrix elements. *Chem. Phys. Lett.*, **249**, 15 (1996).

[70] R.J. Cave, M.D. Newton. Calculation of electronic coupling matrix elements for ground and excited state electron transfer reactions: comparison of the generalized Mulliken–Hush and block diagonalization methods. *J. Chem. Phys.*, **106**, 9213 (1997).

[71] A. Voiytuk, N. Rosch. Fragment charge difference method for estimating donor-acceptor electronic coupling: application to DNA pi-stacks. *J. Chem. Phys.*, **117**, 5607 (2002).

[72] J. Lappe, R.J. Cave, M.D. Newton, I. Rostov. A theoretical investigation of charge transfer in several substituted acridinium ions. *J. Phys. Chem. B*, **109**, 6610 (2005).

[73] R. Parr, W. Yang. *Density-Functional Theory of Atoms and Molecules*, Oxford University Press, New York (1989).

[74] D.P. Chong, O.V. Gritsenko, E.J. Baerends. Interpretation of the Kohn–Sham orbital energies as approximate vertical ionization potentials. *J. Chem. Phys.*, **116**, 1760 (2002).

[75] M.J. Frisch, G.W. Trucks, H.B. Schlegel, G.E. Scuseria, M.A. Robb, J.R. Cheeseman, V.G. Zakrzewski, J.J.A. Montgomery, R.E. Stratmann, B. Mennucci, C. Pomelli, C. Adamo, S. Clifford, J. Ochterski, G.A. Petersson, P.Y. Ayala, Q. Cui, K. Morokuma, P. Salvador, J.J. Dannenberg, D.K. Malick, A.D. Rabuck, K. Raghavachari, J.B. Foresman, J. Cioslowski, J.V. Ortiz, A.G. Baboul, B.B. Stefanov, G. Liu, A. Liashenko, P. Piskorz, I. Komaromi, R. Gomperts, R.L. Martin, D.J. Fox, T. Keith, M.A. Al-Laham, C.Y. Peng, A. Nanayakkara, M. Challacombe, P.M.W. Gill, B. Johnson, W. Chen, M.W. Wong, J.L. Andres, C. Gonzalez, M. Head-Gordon, E.S. Replogle, J.A. Pople. *Gaussian 98*, Gaussian, Inc., Pittsburgh, PA (2001).

[76] M.J.T. Frisch, G.W. Schlegel, H.B. Scuseria, G.E. Robb, M.A. Cheeseman, J.R. Montgomery Jr., J.A. Vreven, T. Kudin, K.N. Burant, J.C. Millam, J.M. Iyengar, S.S. Tomasi, J. Barone, V. Mennucci, B. Cossi, M. Scalmani, G. Rega, N. Petersson, G.A. Nakatsuji, H. Hada, M. Ehara, M. Toyota, K. Fukuda, R. Hasegawa, J. Ishida, M. Nakajima, T. Honda, Y. Kitao, O. Nakai, H. Klene, M. Li, X. Knox, J.E. Hratchian, H.P. Cross, J.B. Bakken, V. Adamo, C. Jaramillo, J. Gomperts, R. Stratmann, R.E. Yazyev, O. Austin, A.J. Cammi, R. Pomelli, C. Ochterski, J.W. Ayala, P.Y. Morokuma, K. Voth, G.A. Salvador, P. Dannenberg, J.J. Zakrzewski, V.G. Dapprich, S. Daniels, A.D. Strain, M.C. Farkas, O. Malick, D.K. Rabuck, A.D. Raghavachari, K. Foresman, J.B. Ortiz, J.V. Cui, Q. Baboul, A.G. Clifford, S. Cioslowski, J. Stefanov, B.B. Liu, G. Liashenko, A. Piskorz, P. Komaromi, I. Martin, R.L. Fox, D.J. Keith, T. Al-Laham, M.A. Peng, C.Y. Nanayakkara, M. Challacombe, P.M.W. Gill, B. Johnson, W. Chen, M.W. Wong, C. Gonzalez, J.A. Pople. *Gaussian 03*, Gaussian Inc., Wallingford, CT (2004).

[77] Cerius 2, 3.5 and 3.7, Molecular Simulations Inc., La Jolla, CA (1997).

[78] M.C. Zerner. ZINDO, 3.7, Molecular Simulations Inc., San Diego, CA, 1991 (1991).

[79] W. Koch, M.C. Holthausen. *A Chemist's Guide to Density Functional Theory*, Wliey-VCH, New York, NY (2001).

[80] B.S. Brunschwig, C. Creutz, N. Sutin. Optical transitions of symmetrical mixed-valence systems in the class II–III Regime. *Chem. Soc. Rev.*, **31**, 168 (2002).

[81] G.M. Brown, F.R. Hopf, J.A. Ferguson, T.J. Meyer, D.G. Whitten. Mettaloporphyrin redox chemistry. The effect of extra planar ligands on the site of oxidation in ruthenium porphyrins. *J. Am. Chem. Soc.*, **95**, 5939 (1973).

[82] A. Dreuw, J.L. Weisman, M. Head-Gordon. Long-range chrage-transfer excited states in time-dependent density functional theory require non-local exchange. *J. Chem. Phys.*, **119**, 2943 (2003).

[83] Z.-L. Cai, K. Sendt, J.R. Reimers. Failure of density-functional theory and time-dependent density-functional theory for large extended pi systems. *J. Chem. Phys.*, **117**, 5543 (2002).

[84] S. van Gisbergen, V. Osinga, O.V. Gritsenko, R. vanLeeuwen, J.G. Snijders, E.J. Baerends. Improved density functional theory results for frequency-dependent polarizabilities, by the use of an exchange-correlation potential with correct asymptotic behavior. *J. Chem. Phys.*, **105**, 3142 (1996).

[85] B. Champagne, E.A. Perpete, S.J.A. v, E.J. Gisbergen, J.G. Baerends, C. Snijders, K.A. Soubra-Ghaoui, B Robins. Assessment of conventional density functional theory schemes for computing the polarizabilities and hyperpolarizabilities of conjugated oligomers: an *ab initio* investigation of polyacetylene chains. *J. Chem. Phys.*, **109**, 10489 (1998).

[86] A.A. Stuchebrukhov. Tunneling currents in electron transfer reaction in proteins. 2. Calculation of electronic superexchange matrix element and tunneling currents using nonorthogonal basis sets. *J. Chem. Phys.*, **105**, 10819 (1996).

[87] A.A. Stuchebrukhov. Tunneling currents in proteins: nonorthogonal atomic basis sets and Mulliken population analysis. *J. Chem. Phys.*, **107**, 6495 (1997).

[88] A.A. Stuchebrukhov. Toward *ab initio* theory of long-distance electron tunneling in proteins: tunneling currents approach. *Adv. Chem. Phys.*, **118**, 1 (2001).

[89] G.S.M. Tong, I.V. Kurnikov, D.N. Beratan. Tunneling energy effects on GC oxidation in DNA. *J. Phys. Chem. B*, **106**, 2381 (2002).

[90] M.V. Basilevsky, G.E. Chudinov, M.D. Newton. The multiconfigurational adiabatic electron-transfer theory and its invariance under transformations of charge-density basis functions. *Chem. Phys.*, **179**, 263 (1994).

[91] M.V. Basilevsky, G.E. Chudinov, I.V. Rostov, Y.P. Liu, M.D. Newton. Quantum-chemical evaluation of energy quantities governing electron transfer kinetics: applications to intramolecular processes. *J. Mol. Struct. (Theochem)*, **371**, 191 (1996).

[92] M.V. Basilevsky, I.V. Rostov, M.D. Newton. A two-dimensional Born-Oppenheimer treatment of intramolecular electron transfer reactions. *J. Electroanal. Chem.*, **450**, 69 (1998).

[93] M.V. Basilevsky, I.V. Rostov, M.D. Newton. A frequency-resolved cavity model (FRCM) for treating equilibrium and non-equilibrium solvation energies. *Chem. Phys.*, **232**, 189 (1998).

[94] M.V. Basilevsky, I.V. Rostov, M.D. Newton. A two-dimensional Born-Oppenheimer treatment of intramolecular electron transfer reactions. *J. Electroanal. Chem.*, **450**, 69 (1998).

[95] H.M. McConnell. Intramolecular charge transfer in aromatic free radicals. *J. Chem. Phys.*, **35**, 508 (1961).

[96] D.N. Beratan. Electron-tunneling through rigid molecular Bridges—Bicyclo[2.2.2]Octane. *J. Am. Chem. Soc.*, **108**, 4321 (1986).

[97] J.F. Stanton, R.J. Bartlett. The equation of motion coupled-cluster method. A systematic biorthogonal approach to molecular excitation energies, transition probabilities, and excited state properties. *J. Chem. Phys.*, **98**, 7029 (1993).

[98] M. Nooijen. Similarity transformed equation of motion coupled-cluster study of excited states of selected azabenzenes. *Spectrochim. Acta Part A Mol. Biomol. Spectrosc.*, **55**, 539 (1999).

[99] I. Daizadeh, E.S. Medvedev, A.A. Stuchebrukhov. Effect of protein dynamics on biological electron transfer. *Proc. Natl. Acad. Sci. USA*, **94**, 3703 (1997).

[100] S.S. Skourtis, I.A. Balabin, T. Kawatsu, D.N. Beratan. Protein dynamics and electron transfer: electronic decoherence and non-condon effects. *Proc. Natl. Acad. Sci. USA*, **102**, 3552 (2005).

[101] G. Jones II, L.N. Lu, H. Fu, C.W. Farahat, C. Oh, S.R. Greenfield, D.J. Gosztola, M.R. Wasielewski. Intramolecular electron transfer across amino acid spacers in the picosecond time regime. Charge transfer interaction through peptide bonds. *J. Phys. Chem. B*, **103**, 572 (1999).